A Frequency Domain Interpretation of Signal Injection Methods for Salient PMSMs

Bowen Yi, Slobodan N. Vukosavić, Romeo Ortega, Aleksandar M. Stanković and Weidong Zhang

Abstract—Several heuristic procedures to estimate the rotor position of interior permanent magnet synchronous motors via signal injection have been reported in the applications literature, and are widely used in practice. These methods, based on the use linear time invariant high-pass/low-pass filters, are instrumental for sensorless controllers. To the best of our knowledge, no theoretical analysis has been carried out for them. The objectives of this note, are (i) to invoke some recent work on the application of averaging techniques for injectionbased observer design to develop a theoretical framework to analyze the sensorless methods, and (ii) to propose a new method that, on one hand, ensures an improved accuracy and, on the other hand, can be related with the current filtering technique. An additional advantage of the new method is that it relies on the use of linear operators, implementable with simple computations. The effectiveness of the proposed scheme is assessed by experiments.

NOMENCLATURE

Symbols

Symbols	
$\alpha - \beta$	Stationary axis reference frame quantities
d-q	Synchronous axis reference frame quantities
n_p	Number of pole pairs
R_s	Stator resistance $[\Omega]$
ω	Angular velocity [rad/s]
Φ	Magnetic flux [Wb]
J	Drive inertia [kg·m ²]
$ au_L$	Load torque [N·m]
f	Friction constant
θ	Rotor flux angle [rad]
L_d, L_q	d and q -axis inductances [H]
v, i	Stator voltage and current [V, A]
ω_h	Angular frequency of injection signal [rad/s]
ε	Period of injection signal $(\varepsilon = \frac{2\pi}{\omega h})$ [s]
V_h	Amplitude of injection signal [V]
s	Laplace transform symbol/ differential operator
$i_{lphaeta}$	$[i_{lpha},i_{eta}]^{ op}$
$v_{\alpha\beta}$	$[v_{lpha},v_{eta}]^{ op}$
I, \mathcal{J}	Identity matrix on $\mathbb{R}^{2\times 2}$ and $\begin{bmatrix} 0 & -1 \\ 1 & 0 \end{bmatrix}$

This paper is supported by the National Natural Science Foundation of China (61473183, U1509211), China Scholarship Council, the Government of Russian Federation (074U01), the Ministry of Education and Science of Russian Federation (14.Z50.31.0031).

B. Yi and W. Zhang are with Department of Automation, Shanghai Jiao Tong University, Shanghai 200240, China (e-mail: yibowen@ymail.com, wdzhang@sjtu.edu.cn). S.N. Vukosavić is with the Electrical Engineering Department, University of Belgrade, Belgrade 11000, Serbia (e-mail: boban@etf.rs). R. Ortega is with L2S, CNRS-CentraleSupélec, Gif-survette 91192, France (e-mail: ortega@lss.supelec.fr). A.M. Stanković is with the Department of Electrical Engineering and Computer Science, Tufts University, Medford, MA 02155 USA (e-mail: astankov@ecc.tufts.edu).

I. Introduction

Permanent magnet synchronous motors (PMSMs) are widely used in industrial applications because of their superior power density and high efficiency. The sensorless control of PMSMs is increasingly attractive for its inherent advantages. Two different types of sensorless control methodologies are reported in the literature. The first type is the model-based method, which is usually known as the back-emf or flux-linkage estimation, utilizing the fundamental components of electrical signals [1], [2], [12], [14]. The second one is saliency-tracking-based method, in which information is extracted from the high-frequency components of stator currents via high-frequency signal injections [7], [9], [10]. The latter, which utilizes the anisotropy due to rotor saliency and magnetic saturation, is favored in the low speed region, where the motor loses observability [10], [14]. In this paper, we address the problem of position estimation for interior PMSMs at low speeds or standstill, thus adopting the second methodology.

The signal injection method is a widely-used techniqueoriented method for electromechanical systems. With the notable exception of [4], [5], [10], no theoretical analysis can be found in the literature. In the last two decades, signal injection-based approaches were developed adopting the following approach¹, first, high frequency probing signals are injected into the motor terminal with the main driving power; then, extract the high-frequency components of the stator currents to get position estimates. Thus, the key problem is the signal processing of the measured stator currents, which is usually achieved via the combination of linear time invariant (LTI) high pass-filters (HPFs) and low-pass filters (LPFs) [13]. Several technique-oriented procedures have been reported in the literature to solve the signal processing problem, however, to the best of our knowledge, no theoretical analysis of these heuristic methods has been reported in the literature. An open problem is providing a theoretical interpretation to the existing technique-oriented methods. The importance of disposing of rigorous analytic results can hardly be overestimated, since it allows, on one hand, to carry out a quantitative performance assessment while, on the other hand, it provides guidelines to make more systematic and simplify the parameter tuning procedure.

The main contributions of our paper are twofold.

• To apply the averaging technique to analyse the mechanism and the estimation accuracy of the *conventional*

¹In this paper, the "classical heuristic" or "technique-oriented" procedures refer to this route.

HPF/LPF procedure quantitatively.

 To utilize the new filtering stage, proposed in [18], to provide new filters selections. Since the proposed scheme also uses linear filters—but, in our case they are time varying—the increase in computational complexity is negligible, also providing a nice downwardscompatibility with the existing approaches.

The remainder of paper is organized as follows. In Section II, we recall the mathematical model of interior PMSMs and formulate the problem. Section III presents the main results, including the interpretation to the conventional methods and a novel design. Simulation and experimental results are given in Section IV and the paper is wrapped-up with some concluding remarks in Section V.

II. MODEL AND PROBLEM FORMULATION

The stationary model of PMSMs, together with the mechanical dynamics, can be expressed as follows [13]

$$L(\theta) \frac{d}{dt} i_{\alpha\beta} = F(i_{\alpha\beta}, \theta, \omega) + v_{\alpha\beta}$$

$$\frac{d}{dt} \theta = n_p \omega$$

$$J \frac{d}{dt} \omega = n_p \Phi(i_{\beta} \cos \theta - i_{\alpha} \sin \theta) - f\omega - \tau_L,$$
(1)

where we define the mappings

$$L(\theta) := L_0 I + L_1 Q(\theta)$$

$$Q(\theta) := \begin{bmatrix} \cos 2\theta & \sin 2\theta \\ \sin 2\theta & -\cos 2\theta \end{bmatrix},$$

and

$$F := (2n_p \omega L_1 Q(\theta) \mathcal{J} - R_s I) i_{\alpha\beta} + n_p \omega \Phi \begin{bmatrix} \sin \theta \\ -\cos \theta \end{bmatrix}.$$

with the averaged inductance $L_0:=\frac{1}{2}(L_d+L_q)$ and the inductance difference value $L_1:=\frac{1}{2}(L_d-L_q)$.

Problem Formulation. Assume there is a stabilizing controller operator Σ_C measuring only $i_{\alpha\beta}$, and define its output as

$$v_{\alpha\beta}^C(t) := \Sigma_C[i_{\alpha\beta}(t)].$$

Inject a high-frequency signal to one axis of the control voltage, say, the α -axis, that is,

$$v_{\alpha\beta} = v_{\alpha\beta}^C + \begin{bmatrix} V_h \sin \omega_h t \\ 0 \end{bmatrix}, \tag{2}$$

where $\omega_h := \frac{2\pi}{\varepsilon}$, with $\varepsilon > 0$ *small*, and $V_h > 0$. We are interested in the following problems.

Q1 Designing an operator $\Sigma_E : i_{\alpha\beta} \mapsto \hat{\theta}$ such that

$$\limsup_{t \to \infty} |\hat{\theta}(t) - \theta(t)| \le \mathcal{O}(\varepsilon), \tag{3}$$

where \mathcal{O} is the uniform big O symbol.²

 $^2{\rm That}$ is, $f(z,\varepsilon)=\mathcal{O}(\varepsilon)$ if and only if $|f(z,\varepsilon)|\leq C\varepsilon,$ for a constant C independent of z and $\varepsilon.$

Q2 Providing a rigorous frequency domain interpretation of the conventional filtering methods.

It is well-known that high frequency probing signals almost have no effects on the motor mechanical coordinates. However, due to the rotor saliency, it induces different high-frequency responses in the α - and β -axes currents. This fact provides the possibility to recover the angle from the high-frequency components of stator currents.

III. MAIN RESULTS

In this section, we give the analysis of frequency decomposition of the stator currents $i_{\alpha\beta}$, which is instrumental for the design and analysis of position estimators.

A. Conventional Frequency Analysis

First we recall the conventional frequency decomposition in the technique-oriented literature, which relies on the *adhoc* application of the superposition law [8], [13]. That is, suppose the electrical states consist of high-frequency and low-frequency components as $(\cdot)_{\alpha\beta} = (\cdot)_{\alpha\beta}^h + (\cdot)_{\alpha\beta}^\ell$. If $\omega \approx 0$, the current responses can be separated as

$$v_{\alpha\beta}^{\ell} + v_{\alpha\beta}^{h} = (R_{s}I + L(\theta)s)(i_{\alpha\beta}^{\ell} + i_{\alpha\beta}^{h}). \tag{4}$$

For the approximate high-frequency model $v_{\alpha\beta}^h \approx L(\theta)s[i_{\alpha\beta}^h]$ neglecting the stator resistance, the angle θ can be regarded as a *constant*, thus the high-frequency response contains the information of θ , namely, for the input (2)

$$i_{\alpha}^{h} = \frac{V_{h}(L_{0} - L_{1}\cos 2\theta)}{L_{d}L_{q}s} \left[\sin \omega_{h}t\right]$$
$$i_{\beta}^{h} = -\frac{(V_{h}L_{1}\sin 2\theta)}{L_{d}L_{q}s} \left[\sin \omega_{h}t\right].$$

Substituting $s = j\omega_h$, we approximately get the high-frequency components of the stator current as

$$i_{\alpha\beta}^{h} = \frac{1}{\omega_{h}L_{d}L_{q}} \begin{bmatrix} L_{0} - L_{1}\cos 2\theta \\ -L_{1}\sin 2\theta \end{bmatrix} (-V_{h}\cos \omega_{h}t).$$
 (5)

The derivation of the above high-frequency model is based on two assumptions, namely, the superposition law and the slow angular velocity $\omega \approx 0$, implying that this decomposition is only applicable at standstill or very low speeds.

B. Frequency Analysis via Averaging

Averaging analysis provides a rigorous and elegant decomposition of the measured currents as follows. We refer the reader to [4], [6], [16], [17] for some basic knowledge on averaging analysis. Applying averaging analysis, it is shown that with ω_h large enough

$$i_{\alpha\beta} = \bar{i}_{\alpha\beta} + \varepsilon y_v S + \mathcal{O}(\varepsilon^2),$$
 (6)

where, we defined the signal

$$S(t) := -\frac{V_h}{2\pi} \cos(\omega_h t), \tag{7}$$

the (so-called) virtual output

$$y_v := \frac{1}{L_d L_q} \begin{bmatrix} -L_1 \cos 2\theta + L_0 \\ -L_1 \sin 2\theta \end{bmatrix}, \tag{8}$$

and $\bar{i}_{\alpha\beta}$ is the current of the closed-loop system with $v_{\alpha\beta} = v_{\alpha\beta}^C$ —that is, without signal injection. From (8) it is clear that

$$\theta = \frac{1}{2} \arctan\left(\frac{y_{v_2}}{y_{v_1} - \frac{L_0}{L_d L_a}}\right). \tag{9}$$

Hence the position estimation problem is translated into the estimation of y_v . Towards this end, we notice that, from a frequency viewpoint, $i_{\alpha\beta}$ contains fundamental frequency components $\bar{i}_{\alpha\beta}$ and high frequency components $\varepsilon y_v S$.

C. Quantitative Interpretation of LTI Filtering Methods

It is natural, then, that to "reconstruct" y_v —out of measurements of $i_{\alpha\beta}$ —we need to separate these components via some sort of HPF and LPF operations. This is the rationale underlying all existing position estimators reported in the literature, see [13] for a recent review. In [13] the position estimation method, for low rotation speeds, shown in Fig. 1 is proposed.

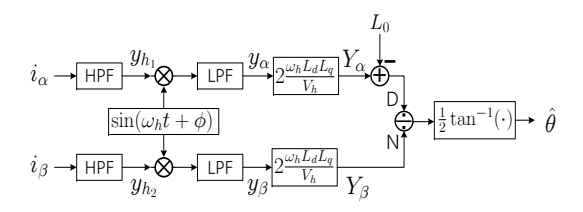


Fig. 1. Block diagram of the conventional signal injection method

To evaluate the performance of the classical method in Fig. 1, without loss of generality, select the LTI filters as

$$\begin{aligned} \text{HPF}(s) &= \frac{2s^2}{(\lambda_h + s)^2} \\ \text{LPF}(s) &= \frac{\lambda_\ell}{\lambda_\ell + s}, \end{aligned} \tag{10}$$

with parameters

$$\lambda_h = \omega_h, \ \lambda_\ell = \max\{\sqrt{\omega_h \omega_\star}, 1\}.$$
 (11)

The Bode diagrams of two filters are given in Fig. 2 with $\omega_h=500,~\omega_\star=1.$

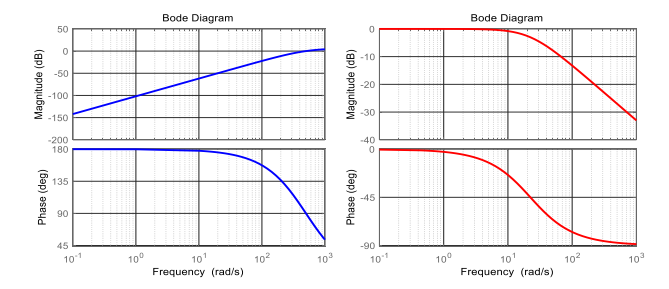


Fig. 2. Bode Diagram of the HPF/LPF (10) ($\omega_h = 500, \ \omega_\star = 1$)

Applying averaging analysis at reduced speeds, and setting $\phi=0$, we have the following proposition. ³

Proposition 1: For the IPMSM dynamics (1), suppose the control that $v_{\alpha\beta}^C$ guarantees all the states bounded with

$$\left| (\bar{\omega}, \dot{\bar{\omega}}, \dot{v}_{\alpha\beta}^C) \right| \le \ell_{\omega}$$

for some constant ℓ_{ω} independent of ε . If the filters are selected as (10)-(11), then the signal processing procedure in Fig. 1, namely,

$$y_h = \text{HPF}[i_{\alpha\beta}]$$

$$\begin{pmatrix} Y_{\alpha} \\ Y_{\beta} \end{pmatrix} = \frac{2\omega_h L_d L_q}{V_h} \cdot \text{LPF}[y_h \times \sin(\omega_h t + \phi)]$$

$$\hat{\theta} = \frac{1}{2} \arctan\left(\frac{Y_{\beta}}{Y_{\alpha} - L_0}\right)$$
(12)

with $\phi = 0$, guarantees

$$\limsup_{t \to \infty} |\hat{\theta}(t) - \theta(t)| = n\pi + \mathcal{O}(\varepsilon^{\frac{1}{2}})$$

for $n\in\mathbb{Z}$, when $\omega_h\geq\omega_h^{\star}$ for some $\omega_h^{\star}\in\mathbb{R}_+$, with $\varepsilon=\frac{2\pi}{\omega_h}$.

Proof: Applying the operator HPF to (6), we have 4

$$\mathrm{HPF}[i_{\alpha\beta}] = \mathrm{HPF}[\bar{i}_{\alpha\beta}] + \frac{2\pi}{\omega_h} \mathrm{HPF}[D(\theta)S] + \mathcal{O}(\varepsilon^2) + \epsilon_t, \tag{13}$$

with the definition

$$D(\theta) := L^{-1}(\theta) \begin{bmatrix} 1 \\ 0 \end{bmatrix}.$$

For the first term of (13), we have

$$\begin{split} \mathrm{HPF}[\bar{i}_{\alpha\beta}] &= \frac{2}{(w_h + s)^2} \bigg[\frac{\partial \mathcal{F}}{\partial \bar{i}_{\alpha\beta}} \cdot (\mathcal{F} + L^{-1} v^C_{\alpha\beta}) + n_p \bar{\omega} \\ &\times \left(\frac{\partial \mathcal{F}}{\partial \bar{\theta}} + \frac{\partial L^{-1}}{\partial \bar{\theta}} v^C_{\alpha\beta} \right) + \left(\frac{\partial \mathcal{F}}{\partial \bar{\omega}} + L^{-1} \right) \mathcal{O}(\ell_\omega) \bigg] \end{split}$$

where we have used the assumption $\left|(\bar{\omega}, \dot{\bar{\omega}}, \dot{v}_{\alpha\beta}^C)\right| \leq \ell_{\omega}$ in the last term, with

$$\mathcal{F}(i_{\alpha\beta}, \theta, \omega) := L^{-1}(\theta) F(i_{\alpha\beta}, \theta, \omega).$$

There always exists a constant $\omega_h^{\star} \in \mathbb{R}_+$ such that for $\omega_h > \omega_h^{\star}$

$$\mathtt{HPF}[\bar{i}_{\alpha\beta}] = \frac{2}{\omega_h^2} \cdot \frac{\omega_h^2}{(\omega_h + s)^2} \big[\mathcal{O}(1) \big].$$

Some basic linear system analysis shows $\left|\frac{\omega_h^2}{(\omega_h + s)^2} [\mathcal{O}(1)]\right| = \mathcal{O}(1)$, thus yielding

$$\mathrm{HPF}[\bar{i}_{\alpha\beta}] = \mathcal{O}(\varepsilon^2).$$

³Indeed, the saliency-tracking-based method has an angular ambiguity of π due to the $\tan^{-1}(\cdot)$ operation. It is possible to utilize the saturation effect in d-axis of machine, as well as y_v to conduct the magnetic polarity identification. The problem is out of the scope of the paper, and we refer the readers to [9], [11] for more details.

 4 We omit the exponentially decaying term ϵ_t of filtered signals in the following analysis.

For the second term in the right hand side of (13), we have

$$\begin{split} \frac{2\pi}{\omega_h} \mathrm{HPF}[D(\theta)S] &= -\frac{2V_h}{\omega_h} \frac{1}{(\omega_h + s)^2} \bigg[a_1(t) \cos(\omega_h t) + a_2(t) \omega_h \\ &\times \sin(\omega_h t) - a_3(t) \omega_h \sin(\omega_h t) - \omega_h^2 D(\theta) \cos(\omega_h t) \bigg]. \end{split}$$

with $a_1(t) := \frac{d}{dt}(n_p\omega D'(\theta))$, $a_2(t) := n_p\omega D'(\theta)$ and $a_3(t) = \omega_h D'(\theta) n_p\omega$, whose derivatives are bounded. When ω_h is large enough, we have

$$\frac{2\pi}{\omega_h} \mathrm{HPF}[D(\theta)S] = \frac{1}{\omega_h} V_h D(\theta) \sin(\omega_h t) + \mathcal{O}(\varepsilon^2).$$

Therefore, the currents filtered by the HPFs become

$$y_h := \text{HPF}[i_{\alpha\beta}] = \frac{1}{\omega_h} V_h D(\theta) \sin(\omega_h t) + \mathcal{O}(\varepsilon^2).$$
 (14)

Multiplying $\sin(\omega_h t + \phi)$ on both sides with $\phi = 0$, we get

$$\sin(\omega_h t) y_h = \frac{V_h}{2\omega_h} D(\theta) - \frac{V_h}{2\omega_h} D(\theta) \cos(2\omega_h t) + \mathcal{O}(\varepsilon^2),$$
(15)

where we have used the trigonometric identity

$$\sin^2 \theta = \frac{1 - \cos 2\theta}{2}.$$

Applying the LPF to (15), for the first term we have

$$\operatorname{LPF}\left[\frac{V_h}{2\omega_h}D(\theta)\right] = \frac{V_h}{2\omega_h}D(\theta) - \frac{V_h}{2\omega_h}\frac{s}{\lambda_\ell + s}\left[D(\theta)\right] \\
= \frac{V_h}{2\omega_h}D(\theta) + \mathcal{O}(\varepsilon^{\frac{3}{2}}).$$

For the second term, we have

$$\mathrm{LPF}\left[\frac{V_h}{2\omega_h}D(\theta)\cos(2\omega_h t)\right] = \mathcal{O}(\varepsilon^{\frac{3}{2}}),$$

with straightforward calculations and the swapping lemma. Therefore, the filtered signal satisfies

$$\begin{bmatrix} y_{\alpha} \\ y_{\beta} \end{bmatrix} := \text{LPF}[\sin(\omega_h t) y_h] = \frac{V_h}{2\omega_h} D(\theta) + \mathcal{O}(\varepsilon^{\frac{3}{2}}).$$

Notice the exact form of $D(\theta)$, thus we having

$$\begin{bmatrix} Y_{\alpha} \\ Y_{\beta} \end{bmatrix} := \begin{bmatrix} \frac{2\omega_h L_d L_q}{V_h} y_{\alpha} \\ \frac{2\omega_h L_d L_q}{V_h} y_{\beta} \end{bmatrix}$$
$$= \begin{bmatrix} L_0 - L_1 \cos 2\theta \\ -L_1 \sin 2\theta \end{bmatrix} + \mathcal{O}(\varepsilon^{\frac{1}{2}}).$$

Therefore, when $t \to \infty$ we have

$$\tan 2\theta = \frac{Y_{\beta}}{Y_{\alpha} - L_0} + \mathcal{O}(\varepsilon^{\frac{2}{2}}).$$

It completes the proof.

A corollary at standstill is given as follows. *Corollary 1:* For Proposition (1) with $\omega \equiv 0$, we have

$$\limsup_{t \to \infty} |\hat{\theta}(t) - \theta(t)| = n\pi + \mathcal{O}(\varepsilon)$$

with $n \in \mathbb{Z}$.

Proof: It follows clearly with $\lambda_{\ell} = 1$.

D. New LTV Filtering Method

In this subsection, we introduce a novel LTI HPF and linear time-varying (LTV) LPF with enhanced steady-state accuracy. The new design is experimentally validated in [20] with its theoretical foundations reported in [18], [19].

Fixing $\phi = \frac{3\pi}{2}$, we propose to select the new filters as

$$\begin{aligned} \text{HPF}: \quad G_d(s) &:= e^{-ds} + \frac{1}{2ds} \left(e^{-2ds} - 1 \right) \\ \text{LPF} &= \frac{1}{2} \left(\frac{V_h}{2\pi} \right)^2 \mathcal{H}, \end{aligned} \tag{16}$$

where \mathcal{H} is the single-input single-output LTV filter

$$\dot{z}(t) = -\gamma S^2(t)z(t) + \gamma u(t)$$

$$\mathcal{H}[u(t)] = z(t),$$
(17)

with $d, \gamma > 0$ —see Fig. 3.

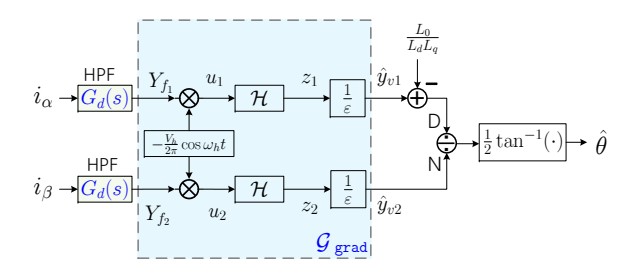


Fig. 3. Equivalent block diagram of the proposed estimation method

The signal processing of the filters described above consists of the following steps.

Step 1) Generate the following filtered signal from the new HPF.

$$Y_f(s) = G_d(s)i_{\alpha\beta}(s).$$

Step 2) Apply the operator \mathcal{G}_{grad} to Y_f in order to generate the estimate of y_v , denoted \hat{y}_v , that is,

$$\hat{y}_v(t) = \mathcal{G}_{\text{grad}}[Y_f(t)], \tag{18}$$

where the LTV operator \mathcal{G}_{grad} is defined as

$$\dot{x}(t) = -\gamma S^{2}(t)x(t) + \gamma S(t)u(t)$$

$$\mathcal{G}_{\text{grad}}[u(t)] = \frac{1}{\varepsilon}x(t).$$
(19)

Step 3) Use the relation (9) to get the position estimate.

Regarding the new filters design, we have the following proposition.

Proposition 2: For the IPMSM dynamics (1), suppose the control $v_{\alpha\beta}^C$ guarantees all states are bounded, with y_v defined in (8) verifying

$$|\dot{y}_v| \le \ell_v,\tag{20}$$

for some constant ℓ_v , and select with $d=\varepsilon$. Then, there exist constants $\omega_h^\star, \gamma^\star > 0$ such that for $\omega_h > \omega_h^\star$ and $\gamma > \gamma^\star$, the estimate satisfies

$$\limsup |\mathcal{G}_{\text{grad}}^{\gamma} \circ G_d(s)[i_{\alpha\beta}(t)] - y_v(t)| = \mathcal{O}(\varepsilon).$$

Proof: The proof follows directly from Proposition 3 in [18].

E. Discussions

- **D1** The dynamics (1) is highly nonlinear. It is well-known that nonlinear systems "mix" the frequencies, making the superposition law not applicable. Although using the *classical* decomposition (4) to estimate position may work in practice, it fails to reliably provide, neither a framework for a quantitative performance assessment, nor guidelines to tune parameters.
- **D2** It should be noticed that the high frequency term $\varepsilon y_v S$ in (6) coincides with the one in (5), but the averaging analysis characterizes all the components in $i_{\alpha\beta}$ quantitatively.
- **D3** To the best of the authors' knowledge, Proposition 1 provides the first quantitative analysis of conventional LTI filtering methods with signal injection reported in the literature.
- **D4** From Propositions 1 and 2 it is clear that the steady-state accuracy of the new LTV filters design is higher than the one of conventional LTI filtering methods.

IV. SIMULATIONS AND EXPERIMENTS

A. Simulations

The proposed estimator is first tested by means of simulations in Matlab/Simulink. We use the parameters of Table I, the current-feedback controller Σ_C given below, together with the proposed estimator.

- 1) Position estimator in Fig. 2 (LTV and LTI designs).
- 2) Rotation between $\alpha\beta$ -coordinates and misaligned dq-coordinates, namely, $i_{dq}=e^{-\mathcal{I}\hat{\theta}}i_{\alpha\beta},\ v_{\alpha\beta}=e^{\mathcal{I}\hat{\theta}}v_{dq}.$
- 3) Speed regulation PI loops

$$i_{dq}^{\star} = \left(K_p + K_i \frac{1}{s}\right) (\omega^{\star} - \hat{\omega}),$$

where ω^{\star} is the reference speed, and $\hat{\omega}$ is an estimate of the rotor speed obtained via the following PLL-type estimator.

$$\dot{\eta}_1 = K_p(\hat{\theta} - \eta_1) + K_i \eta_2
\dot{\eta}_2 = \hat{\theta} - \eta_1
\dot{\omega}_p = K_p(\hat{\theta} - \eta_1) + K_i \eta_2
\dot{\omega} = \frac{1}{\eta_p} \hat{\omega}_p.$$
(21)

4) Current regulation loops

$$\begin{split} v_d &= \left(K_p + K_i \frac{1}{s}\right) (i_d^{\star} - i_d^{\ell}) - L n_p \hat{\omega} i_q \\ v_q &= \left(K_p + K_i \frac{1}{s}\right) (i_q^{\star} - i_q^{\ell}) + L n_p \hat{\omega} i_d + n_p \hat{\omega} \Phi, \end{split}$$

where i_{dq}^{ℓ} are filtered signals of i_{dq} by some LPFs.

We operate the motor at the slow speed of 30 rad/min with $\tau_L=0.5~{\rm N\cdot m}$ and the parameters $\varepsilon=10^{-3},~\gamma=10^{-4},~V_h=1,~\omega^\star=0.5$ and those in Table. II. Fig. 4 shows the simulation results. In Fig. 4(a), we also give the position estimate obtained from the conventional LTI filters, denoted as $\hat{\theta}_{\rm LTI}$. Considering the root-mean-square

deviation (RMSD) RMSD = $\sqrt{\frac{1}{t_2-t_1}}\int_{t_1}^{t_2}|\hat{\theta}(s)-\theta(s)|^2ds$ with $\theta,\hat{\theta}\in\mathcal{S}^1$, we calculate the RMSDs for two methods in the interval [5,10] s. They are 0.0872 and 0.1411 for the proposed design and the conventional LTI filtering method, respectively. We conclude that the new design outperforms the conventional LTI filtering method with a higher accuracy. It is also observed that the sensorless control law regulates the angular velocity at the desired value.

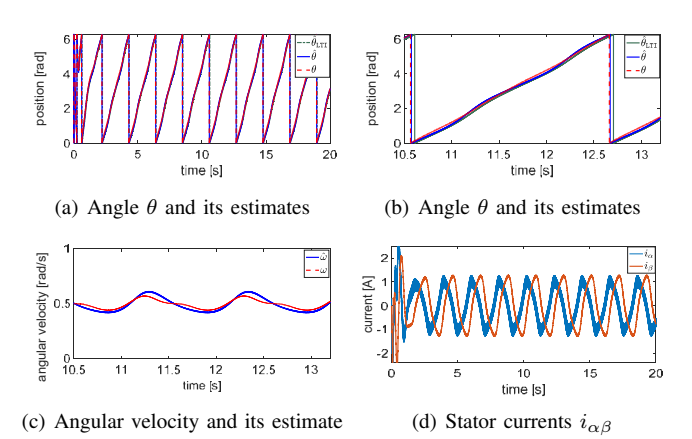


Fig. 4. Simulation results

B. Experiments

System Configuration. The scheme developed in this paper was tested on an interior PMSM platform, shown in Fig. 5. The test IPMSM is a FAST PMSM, whose parameters are given in Table I. It has a 72 V line-to-line peak at 1000 RPM. The voltage of DC bus is 521 V, with the frequency of PWM 5 kHz.

The experimental setup comprises two synchronous motors with surface-mounted permanent magnets on the rotor. One of them runs in the speed control mode, and it is used to maintain the speed at the desired level. The motors are coupled by means of a toothed belt, which also connects an

TABLE I
PARAMETERS OF THE PMSM: SIMULATION (FIRST COLUMN) AND
EXPERIMENTS (SECOND COLUMN)

Number of pole pairs (n_p)	6	3
PM flux linkage constant (Φ) [Wb]	0.11	0.39
d -axis inductance (L_d) [mH]	5.74	3.38
q -axis inductance (L_q) [mH]	8.68	5.07
Stator resistance (R_s) $[\Omega]$	0.43	0.47
Drive inertia (J) [kg·m ²]	0.01	≥ 0.01

 $\label{thm:table II} \textbf{Parameters of the controller and the PLL estimator}$

$[K_p, K_i]$ in the speed loop	[1, 5]
$[K_p, K_i]$ in the current loop	[5, 5]
$[K_p, K_i]$ in the PLL estimator	[5, 0.01]

inertial wheel. More details on the experimental set-up may be found in [20].



Fig. 5. Experimental testing setup

Experimental Results. In the experiment, the amplitude of the test signal is 2 V, with the frequency 400 Hz. The parameters of the estimator are selected as $\gamma_{\alpha}=1.25\times10^4$ and $\gamma_{\beta}=2.5\times10^4$. For such a case, Fig. 6(a) shows the performance of the proposed position estimator. The test signal was only injected to the α axis, which is illustrated in Fig. 6(b) after Clarke transform. The experimental results show that the new design performs very well.

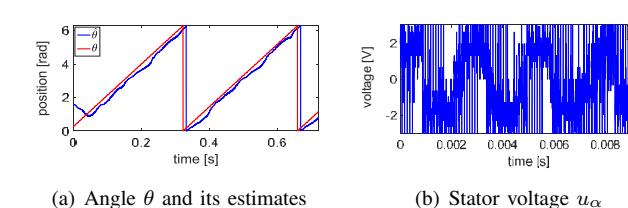


Fig. 6. Experimental results

V. CONCLUSION

This paper addresses the problem of position estimation of IPMSMs at low speeds and standstill. Although the salience-tracking-based methods are effective and widely-studied, the theoretical analysis of the conventional methods, taking into account the nonlinear dynamics of PMSMs, was conspicuous by its absence. This paper attempts to fill in this gap analysing the stator current $i_{\alpha\beta}$ via the averaging method, with guaranteed error with respect to the injection frequency ω_h . Also, with the key identity (6), we develop a new position estimator, which ensures an improved accuracy. Moreover, we establish the connection between the new method and the conventional one, showing that they can be unified in the HPF/LPF framework from the perspective of signal processing.

The following extension and issues are of interest to be further explored.

- For the sake of clarity, we only study the basic case of signal-injection methods for the IPMSM model (1).
 The proposed method can also be extended to other motor models, for instance, saturated interior (or surface mounted) PMSMs [10].
- If is of interest to couple the proposed method with some model-based (non-invasive) techniques, for instance the gradient descent observer in [14], in order

to be able to operate sensorless controller over a wide speed range. Such an approach has been pursued in [3], [15]. We underscore that the first globally exponentially convergent solution to sensorless observers design for IPMSMs, applicable to both high/middle and low speeds, is given in [15].

REFERENCES

- [1] P. P. Acarnley, and J. F. Watson, "Review of position-sensorless operation of brushless permanent-magnet machines," *IEEE Trans. Industrial Electronics*, vol. 53, pp. 352-362, 2006.
- [2] A. A. Bobtsov, A. A. Pyrkin, R. Ortega, S. N. Vukosavic, A. M. Stankovic, and E. V. Panteley, "A robust globally convergent position observer for the permanent magnet synchronous motor," *Automatica*, vol. 61, pp. 47-54, 2015.
- [3] J. Choi, K. Nam, A. Bobtsov, and R. Ortega, "Sensorless control of IPMSM based on regression model," *IEEE Trans. Power Electronics*, 2018, (to be published).
- [4] P. Combes, A. K. Jebai, F. Malrait, P. Martin, and P. Rouchon, "Adding virtual measurements by signal injection," in *American Control Conf.* (ACC), 2016, pp. 999-1005.
- [5] P. Combes, F. Malrait, P. Martin, and P. Rouchon, "An analysis of the benefits of signal injection for low-speed sensorless control of induction motors," in *International Symp. on Power Electronics*, Electrical Drives, Automation and Motion, 2016, pp. 721-727.
- [6] J. Hale, Ordinary Differential Equations. New York: Krieger, Huntington, 1980.
- [7] J. Holtz, "Sensorless control of induction machines: With or without signal injection?" *IEEE Trans. Industrial Electronics*, vol. 55, pp. 7-30, 2006.
- [8] J. H. Jang, S. K. Sul, J. I. Ha, K. Ide, and M. Sawamura, "Sensorless drive of surface-mounted permanent-magnet motor by high-frequency signal injection based on magnetic saliency," *IEEE Trans. Industry Applications*, vol. 39, pp. 1031-1039, 2003.
- [9] J. H. Jang, J. I. Ha, M. Ohto, K. Ide, and S. K. Sul, "Analysis of permanent-magnet machine for sensorless control based on highfrequency signal injection," *IEEE Trans. Industry Applications*, vol. 40, pp. 1595-1604, 2004.
- [10] A. K. Jebai, F. Malrait, P. Martin, and P. Rouchon, "Sensorless position estimation and control of permanent-magnet synchronous motors using a saturation model," *International Journal of Control*, vol. 89, pp. 535-548, 2016.
- [11] Y. S. Jeong, R. D. Lorenz, T. M. Jahns, and S. K. Sul, "Initial rotor position estimation of an interior permanent-magnet synchronous machine using carrier-frequency injection methods," *IEEE Trans. Industry Applications*, vol. 41, pp. 38-45, 2005.
- [12] N. Matsui, "Sensorless PM brushless DC motor drives," *IEEE Trans. Industrial Electronics*, vol. 43, pp. 300-308, 1996.
- [13] K. H. Nam, AC Motor Control and Electric Vehicle Application. Boca Raton: CRC Press, 2010.
- [14] R. Ortega, L. Praly, A. Astolfi, J. Lee, and K. Nam, "Estimation of rotor position and speed of permanent magnet synchronous otors with guaranteed stability," *IEEE Trans. Control Systems Technology*, vol. 19, pp. 601-614, 2011.
- [15] R. Ortega, B. Yi, K. Nam and J. Choi, A globally exponentially stable position observer for interior permanent magnet synchronous motors, submitted to *Automatica*, 2019. arXiv: 1905.00833
- [16] J. A. Sanders, F. Verhulst, and J. Murdock, Averaging Methods in Nonlinear Dynamical Systems. New York: Springer, 2007.
- [17] B. Yi, R. Ortega, and W. Zhang, "Relaxing the conditions for parameter estimation-based observers of nonlinear systems via signal injection," Systems & Control Letters, vol. 111, pp. 18-26, 2018.
- [18] B. Yi, R. Ortega, H. Siguerdidjane, and W. Zhang, "An adaptive observer for sensorless control of the levitated ball using signal injection," in *IEEE Conf. on Decision and Control*, Miami Beach, FL, US, Dec. 17-19, 2018.
- [19] B. Yi, R. Ortega, H. Siguerdidjane, J.E. Machado, and W. Zhang, "On generation of virtual outputs via signal injection: Application to observer design for electromechanical systems," *LSS-Supelec, Int Report*, 2018. arXiv:1807.10178
- [20] B. Yi, S.N. Vukosavic, R. Ortega, A.M. Stankovic, W. Zhang, "A new signal injection-based method for estimation of position in interior permanent magnet synchronous motors," under review, 2018.

 $^{^5 \}text{The superscript}$ of the parameter γ denotes the values for the different axes.